Turkish Journal of Electrical Engineering & Computer Sciences

http://journals.tubitak.gov.tr/elektrik/

Research Article

Turk J Elec Eng & Comp Sci
(2020) 28: 61 – 79

doi:10.3906/elk-1904-180

A hybrid model based on the convolutional neural network model and artificial bee colony or particle swarm optimization-based iterative thresholding for the detection of bruised apples

Mahmut HEKIM[1], **Onur COMERT**[2,*], **Kemal ADEM**[3]
[1]Department of Electrical and Electronics Engineering, Faculty of Engineering,
Tokat Gaziosmanpasa University, Tokat, Turkey
[2]Department of Mechatronics Engineering, Faculty of Engineering,
Tokat Gaziosmanpasa University, Tokat, Turkey
[3]Department of Management Information Systems, Faculty of Engineering, Aksaray University, Aksaray, Turkey

Received: 26.04.2019 • **Accepted/Published Online:** 26.10.2019 • **Final Version:** 27.01.2020

Abstract: In this study, apple images taken with near-infrared (NIR) cameras were classified as bruised and healthy objects using iterative thresholding approaches based on artificial bee colony (ABC) and particle swarm optimization (PSO) algorithms supported by a convolutional neural network (CNN) deep learning model. The proposed model includes the following stages: image acquisition, image preprocessing, the segmentation of anatomical regions (stem-calyx regions) to be discarded, the detection of bruised areas on the apple images, and their classification. For this aim, by using the image acquisition platform with a NIR camera, a total of 1200 images at 6 different angles were taken from 200 apples, of which 100 were bruised and 100 healthy. In order to increase the success of detection and classification, adaptive histogram equalization (AHE), edge detection, and morphological operations were applied to the images in the preprocessing stage, respectively. First, in order to segment and discard the stem-calyx anatomical regions of the images, the CNN model was trained by using the preprocessed images. Second, the threshold value was determined by means of the ABC/PSO-based iterative thresholding approach on the images whose stem-calyx regions were discarded, and then the bruised areas on the images with no stem-calyx anatomical regions were detected by using the determined threshold value. Finally, the apple images were classified as bruised and healthy objects by using this threshold value. In order to illustrate the classification success of our approaches, the same classification experiments were reimplemented by directly using the CNN model alone on the preprocessed images with no ABC and PSO approaches. Experimental results showed that the hybrid model proposed in this paper was more successful than the CNN model in which ABC- and PSO-based iterative threshold approaches were not used.

Key words: Bruised apple, stem-calyx, convolutional neural network, artificial bee colony, particle swarm optimization

1. Introduction

Fruit juices are obtained mechanically from healthy, mature, fresh, and clean fruits in order to be resistant to physical deterioration, and in this way, some original features of fruits such as taste, smell, and color can be saved in fruit juices for a long time. Many types of fruit are converted into fruit juices by means of fabrication since they are more resistant to physical deterioration and can be preserved for a longer period of time. In this way, they can be stored as other products that contain the original properties of fruits such as taste, smell, and color. Fruit juices can be divided into three groups as clear fruit juices, cloudy fruit juices, and nectars. Clear

*Correspondence: onur.comert@gop.edu.tr

fruit juices are made of sour cherries, grapes, apples, and pomegranates. However, these fruit types should be healthy, mature, fresh, and clean. In the preparation process of the fruits for the production of fruit juice, they are washed in order to remove the dust, soil, leaves, and broken pieces of fruits to be converted into fruit juice. Then quality control workers on conveyor belts separate the fruits into bruised, healthy, crushed, or raw forms [1]. However, in the separation process, it is difficult to achieve a complete standard due to time and human factors as a large number of fruits will be separated by workers. Therefore, automatic separation processes carried out by machines using image processing technology are of importance in order to speed up the process, reduce costs, and minimize errors [2]. Image processing devices and software are required to use image processing technology.

One of the most important factors that complicate the detection of bruises in apples is the confusion of the stem-calyx of the apple's own anatomical regions with the bruised areas. Therefore, in studies conducted in the literature, images are either taken in such a way that the stem-calyx regions of apples are not visible, or detection and removal of the stem-calyx regions from the images are emphasized primarily. One work [3] involved a study on the recognition of the stem and calyx regions of apples using shape recognition on 600 different color images. The authors used multiple thresholding for the segmentation and extracted the shape features using multifractal, Fourier, and radon identifiers on the objects obtained in this stage. They tested these features on support vector machine (SVM), artificial neural network (ANN), k-nearest neighborhood (k-NN), linear discriminant classifier (LDC), and AdaBoost classifiers and distinguished the stem-calyx regions of apples from the bruised areas with 94% accuracy using the SVM classifier. Other authors [4] conducted a study on the detection of apple diseases using color, texture, and shape-based features. They used L*a*b* color space in the segmentation of the defects on the apple's surface and took 320 apple images with 4 class labels with different diseases as the dataset. They identified the bruised fruit areas with the help of k-means clustering; extracted the color, texture, and shape-based features from the segmented images; and classified the apples as bruised or healthy with an accuracy of 95.95% by using a SVM-based classifier. Other authors [5] conducted a study on fruit detection using the faster R-CNN model. They tested the performance of the system on seven different fruits using both NIR and RGB images. The training time for each fruit was 4 h with the NVIDIA GPU, and as a result, they were able to identify the fruits in the images with an accuracy rate of 83%. One study [6] used faster R-CNN on tomato images for the detection of the location and type of diseases and pests. The authors acquired approximately 5000 images of different sizes and different resolutions of tomatoes and used the data augmentation (DA) method to increase and diversify the training dataset. Of the dataset, 80% was used for training, 10% for validation, and 10% for testing. Their experimental studies showed that the DA method increased the success rate by 35%. As a result of the tests, they identified diseases and pests with accuracy rates in the range of 83% to 90%. Other authors [7] conducted a study on the detection of bruises of apples using histogram-based automatic thresholding. They obtained images from a total of 120 apples of 4 types taken at 730-nm wavelength using structured illumination reflective imaging. Since the apples were in horizontal positions in the images, their stem-calyx regions were not visible. They applied median filter, automatic thresholding, opening, and filling to the images, respectively. They tried 9 different automatic thresholding methods on the images during the thresholding step and found that intermode, Ridler, and Otsu techniques had total correct classification (TCC) success with accuracy of 90%. They found that the false positive (FP) and false negative (FN) rates were the lowest at 6.7% on average with the Ridler technique, and this rate decreased to 5.8% when unimode and Ridler techniques were used together. Other authors [8] classified apples using optical features and SVM according to the level of bruises. They used 155 Fuji-type apples and

took tissue samples of 3 mm in thickness and 2 cm in diameter from these apples using a microtome, and then measured the permeability and reflectivity of the samples at wavelengths of 400-1050 nm with the Integration Sphere System (ISS). They achieved a TCC success rate of 92.5% by applying the obtained features to the SVM. Another work [9] used different ANN models to predict the bruise volumes of apples. The authors applied the measured and predicted test data to the proposed ANN model. From statistical analysis, they found that the predicted test data had a confidence level of 95%. In addition, many studies with successful results in the literature showed that optimization algorithms such as particle swarm optimization (PSO) and artificial bee colony (ABC) were used for iterative thresholding on images [10–13]. The studies that focused on the detection of bruised apples in the literature are presented in Table 1.

Table 1. The studies in the literature.

Author	Year	Objective	Method
Xing and De Baerdemaeker [14]	2005	Detection of bruises in apples	Smoothing, thresholding, hyperspectral
Mohana and Prabhakar [3]	2015	Recognition of stem and calyx regions in apples	Multifractal, Fourier, and radon conversions; SVM, ANN, k-NN, LDC, and AdaBoost classifiers
Dubey and Jalal [4]	2016	Image processing solution for automatic recognition of apple defects	L*a*b* and HSV color spaces, k-means clustering, SVM
Sa et al. [5]	2017	Fruit detection in the NIR and RGB images	Faster R-CNN
Lu and Lu [7]	2017	Detection of bruises in apples	Hyperspectral imaging, opening and filling operations, intermode, Ridler, unimode, and Otsu thresholding
Zhang et al. [8]	2017	Classification according to the level of bruises in apples	SVM, hyperspectral imaging

In this study, apple images taken with near-infrared (NIR) cameras are classified as bruised and healthy objects using iterative thresholding based on ABC/PSO algorithms supported by a convolutional neural network (CNN) model. As a result of the literature survey, although many studies focused on optimization algorithms such as ABC and PSO used for iterative thresholding on images, an ABC/PSO-based iterative thresholding hybrid model supported by a CNN model for analysis of bruised areas in apples is used here for the first time. We investigate the impact of these optimization algorithms supported by a CNN model in the detection of bruised areas and the stem-calyx anatomical regions in apple images, and the classification of apples as bruised or healthy by using the detected threshold value. For this aim, the apple images are enhanced using adaptive histogram equalization (AHE), edge detection, and morphological operations; a CNN model is trained using the enhanced images for the determination of stem-calyx anatomical regions of the apples; these anatomical regions determined by the CNN model are discarded from the images; the bruised areas in the images are detected by using the threshold value determined by means of PSO/ABC-based iterative thresholding; and then the apples are classified as bruised or healthy by using the detected threshold value. Figure 1 shows the application steps of the proposed model in detail.

As shown in Figure 1, the apple images were first enhanced by using AHE, edge detection, and morphological operations. The stem-calyx anatomical regions of the images were then detected by using the trained CNN model and discarded from the images. Then the bruised areas in the images were detected by the threshold value determined by using PSO/ABC-based iterative thresholding. Finally, the apple images with bruised areas were classified as bruised objects and the others as healthy objects.

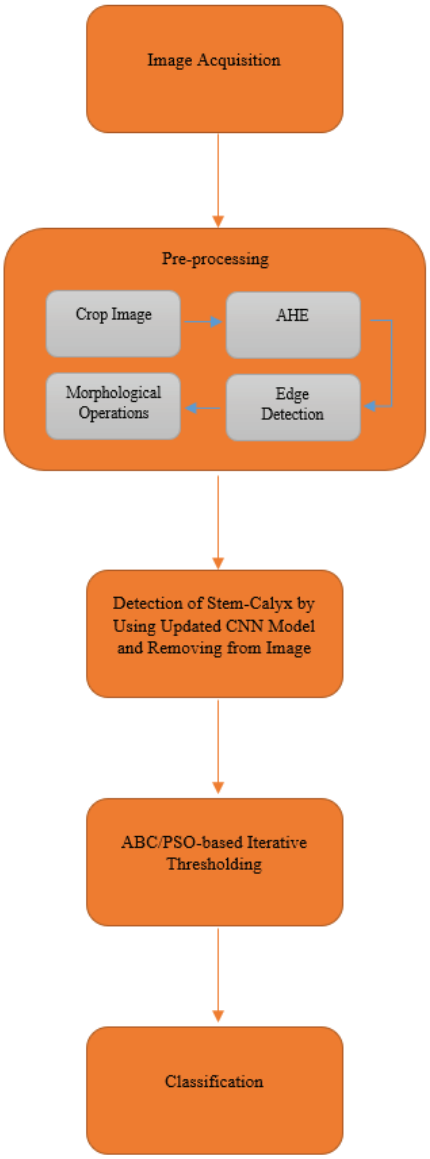

Figure 1. Application steps of the proposed model.

The most important contribution of this study to the literature is that a hybrid model consisting of the CNN model and PSO/ABC-based iterative thresholding approach is used for the first time in the detection of bruised areas in the images. The ABC and PSO algorithms are simple but effective models that can be easily applied to any kind of optimization problem. Although they can be initialized by the same conditions and use the same objective function, they have very different search characteristics. These search characteristics allow discoveries at different levels by using different selection and search operators and thus have high performances for the optimization [13, 15]. Therefore, we examined the capabilities of iterative thresholding of the PSO and ABC algorithms since they are two heuristic algorithms frequently compared in the literature and illustrated to be used for the detection of bruised apples in a hybrid way with the CNN model [13, 16].

2. Apple image dataset

In the image acquisition stage, an image acquisition platform made of 18-mm-thick chipboard material of 40 x 50 x 25 cm in size was used. The platform included a C-mount 6-mm lens (Fujinon HF6HA-1B) and a NIR camera (Teledyne DALSA G3-GM12-M1930) with 2592 x 2048 resolution. The platform was designed to prevent the ambient light from reaching the apple. Two 100-W tungsten-halogen lamps with a wide wavelength range were used as the light source. Figure 2 shows the stage section of the platform.

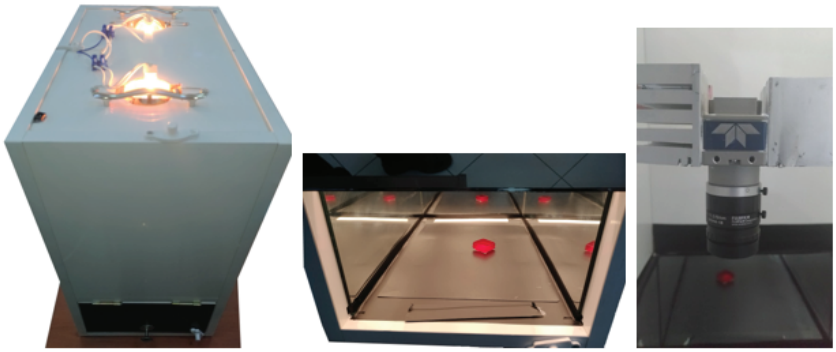

Figure 2. The image acquisition platform.

As shown in Figure 2, there are mirrors on the inner surfaces of the platform that allow the light from the illumination source to fall evenly over the entire surface of the apple. In this way, the shadowing that may form on the apple surface is minimized. A homogeneous black coating was used on the base of the platform to allow distinguishing the apple from the background easily during image processing.

In this study, bruised and healthy samples from widely grown apple varieties in Turkey were collected to create an image dataset. Images were taken at a distance of 15 cm with resolution of 2592 x 2048 pixels. A total of 200 apples were used in the dataset, 100 of them bruised and 100 healthy, and a total of 1200 images were taken from 6 different angles for each apple. In a total of 1200 images, 450 images had bruised areas, whereas 750 had no bruises. For this reason, 450 images were labeled as bruised and 750 images were labeled as healthy by an expert. Similarly, the stem-calyx regions are visible in 960 of the 1200 images and not visible in 240 images. Figure 3 shows the raw apple images without preprocessing.

Figure 3. Raw apple images without preprocessing: (a) healthy apple, (b) bruised apple.

3. Bruise detection using the hybrid model based on the CNN model and ABC/PSO-based iterative thresholding

In this study, first, preprocessing stages, which are the cropping, AHE, edge detection, and morphological operations, were applied to all apple images for the enhancement of them, and then the CNN model was used for the detection of the stem-calyx regions. Finally, ABC/PSO-based iterative thresholding approaches were used for detecting the bruised areas in apple images. Figure 4 shows the procedural steps of our approach.

As shown in Figure 4, the proposed CNN architecture was trained with the faster R-CNN model. CNN was used only for the detection of stem-calyx anatomical regions of the apple images. First of all, the purpose of detecting the stem-calyx regions is to avoid possible confusion due to the morphological similarities of the apple with the bruised areas. As can be seen in Figure 4, after the anatomical regions were detected by using the CNN model and removed from the image, the bruised areas of images were detected by using ABC/PSO-based iterative thresholding. The purpose of applying iterative thresholding methods is to more accurately detect the bruised areas of different apples with different densities and brightnesses. In this study, the CNN model with ABC or PSO approach was constructed in a hybrid structure, where the CNN part of this hybrid structure detected the stem-calyx regions and another part of the structure, ABC or PSO, detected the bruised areas of the images with no stem-calyx regions detected by the part of CNN.

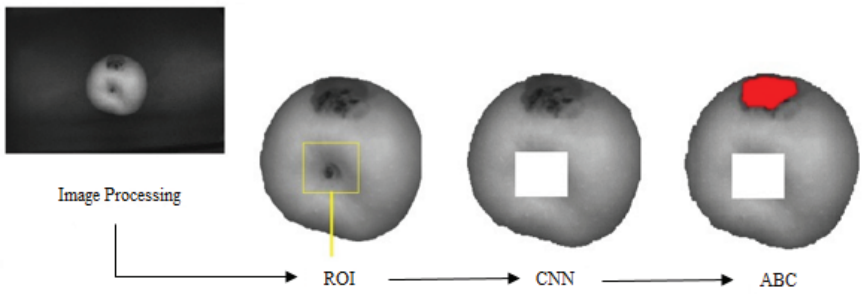

Figure 4. Procedural steps of the proposed approach.

3.1. The enhancement of images using preprocessing techniques

In the preprocessing stage, in order to increase the detection success of the bruised areas and the classification success of apples, we applied adaptive histogram equalization (AHE), Prewitt edge detection, and morphological operations to the raw apple images. Figure 5 shows the enhanced images obtained by using the preprocessing techniques: a) the raw apple image without preprocessing techniques; b) the cropped parts discarded from the image; c) the segmentation of apple and its background using AHE, Prewitt edge detection, and opening-closing operations, where the background was converted to completely white; and d) the erosion process applied to the binary image for removing dark pixels, which occurred due to shadings on the apple's edges, to prevent the confusion of these parts with bruises.

In the experiments, it will be seen that the image preprocessing techniques increase the detection success of the bruised areas and the classification success of apples.

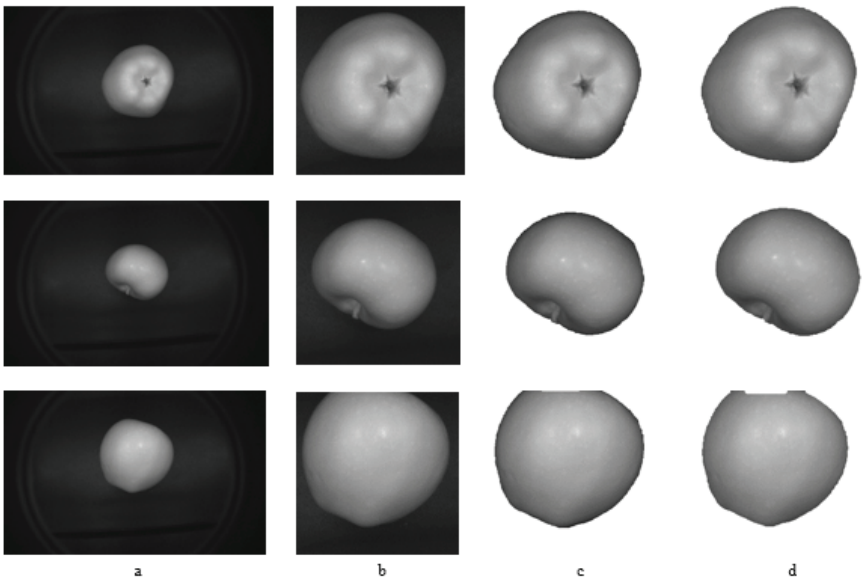

Figure 5. The images obtained by using preprocessing techniques.

3.2. Detection of stem-calyx anatomic regions using the CNN model

The CNN model was inspired by human vision perception. In the first layers, lower-level attributes are learned, whereas in the other layers, higher-level attributes that form certain parts of the object are learned. A typical CNN architecture consists of a fixed-size input layer, convolution layers, pooling (subsampling) layers, and fully connected layers. Each layer plays a different role in the CNN architecture. While the convolution layer extracts features, the fully connected layer allows the classification to be performed on these features. In the pooling layer, the maximum or average of the values adjacent to the feature maps are taken. Thus, the operations are accelerated and the size is reduced in this way. Although the pooling layer reduces the training time, it can also cause information loss. After being processed with multiple convolution and pooling layers, the matrices obtained are directed to fully connected layers and the parameters and weights are learned by functions such as Softmax/RBF [17]. Table 2 shows the parameters of the CNN models used in the study.

Table 2. The CNN models used in the study.

	CNN model		Updated CNN model	
Input image size	32 x 32 x 3		600 x 600 x 3	
Filter number	32		64	
Filter size	3 x 3		3 x 3	
Conv1	Stride=1	Padding=1	Stride=4	Padding=2
Conv2	Stride=1	Padding=1	Stride=4	Padding=2
Max pooling	Pool Size=3	Stride=2	Pool Size=3	Stride=2
Fully connected	64		16	

As shown in Table 2, two different CNN models were used to determine the anatomical structures in apple images. When the parameters used in these two models are evaluated, in the CNN model proposed in this study, the input image size of 600 x 600 pixels and 64 filters allow more clear recognition of the regions that need to be distinguished in the image. The bigger the image size, the longer the training time, but the success does not increase with increasing size. For this reason, the optimum image size was determined as 600 x 600 in accordance with the implemented experimental studies. The convolution layer, which is the first layer in the CNN model used to extract the features, takes its input from the stem-calyx regions labeled on the apple images. In the proposed model, the convolution layers use a convolution core with 4 strides, 2 paddings, and 3 x 3 filter size. When the filter size used in convolution core is too small, the complexity of the extracted features pushes the hardware to its limits, whereas when it is too large, the areas to be detected cannot be identified well. Therefore, to improve the CNN's performance, it is important to use appropriate parameters [18, 19]. In the max pooling layer, which is the subsampling layer, the maximum value of the subregions is taken according to the predetermined scale (pool size) value of 3. This value was set to 3 in this study because a higher value of the scale value may cause the feature size to reduce too quickly, leading to diminished image attributes. The CNN architecture optimizes weights by learning filters on each layer by backpropagation method. This allows the extraction of the distinguishing features of the input image [20]. In the updated faster R-CNN model proposed in this study, the input image size is taken as 600 x 600 pixels. By adjusting the input image size to a higher value than the faster R-CNN model, it was also possible to detect the regions of interest in apple images whose anatomic regions were not completely clear. 6Sixty-four different 3 x 3 filters with 4 strides and 2 paddings were applied in the first and second convolution layers of the updated faster R-CNN model. The number of filters was increased to 64 in order to obtain detailed information about the image compared to the other model. The number of steps was set to 4 to avoid hardware shortage as the size of the entered image and the number of filters increased. The padding size was also determined to 2 for better detection of the anatomical regions corresponding to the corner regions of the images. The accuracy of the classification process was increased by determining the number of fully connected layers to be 16. This value was reduced from 64 to 16 since the number of anatomical regions to be detected in the apple images was small. During the optimization of the weights, the mass size was 64, momentum was 0.85, and weight reduction was 0.001.

3.3. Bruise detection using iterative threshold algorithms

An optimal threshold value is needed to convert a gray-level image to a binary image with minimal loss of information. This value can be found manually by trial and error or it can be calculated using an iterative algorithm. In the literature, in order to perform iterative thresholding, in addition to algorithms such as Otsu [21], swarm optimization algorithms such as ABC and PSO have been used [10–13]. In this study, we performed the thresholding process using ABC and PSO algorithms to determine the bruises. How these algorithms are used for thresholding is described in detail in the following sections.

3.3.1. ABC-based iterative thresholding approach

The ABC algorithm, inspired by the intelligent search behavior of honeybees, is a global optimization and metaintuitive algorithm developed by Karaboga in 2005 in order to optimize numerical problems. It uses only three control parameters predetermined by the user, which are population size, maximum iteration number, and limit [22]. This method has been used for optimization in different areas [23–26]. The steps of the ABC-based iterative thresholding approach are listed as follows:

Step 1: In the gray-scale apple image of 600 x 600 pixels with the stem-calyx parts removed, all food source vectors are set to their initial positions by scout bees. Each x_m refers to a pixel in the apple image:

$$x_{mi} = l_i + rand\,(0,1)\,(u_i - l_i)\,, \tag{1}$$

where the x_{mi} parameter can take a value between l_i and u_i, which are the maximum and minimum values, respectively. l_i and u_i values were determined as 1 and 600 for each apple image.

Step 2: Employed bees seek better food sources (v_m) in their neighborhood. They use the following equation to determine the food sources in their neighborhood:

$$v_{mi} = x_{mi} + \varnothing_{mi}\,(x_{mi} - x_{ki})\,, \tag{2}$$

where i is a randomly selected parameter, x_k is a randomly selected food source, and $\varnothing_{mi}$ is a random number in the [–a, a] range. In this way, a new food source (v_m) is detected and its fitness value is calculated, and a greedy selection is made between x_m and v_m. The fitness values of the pixels in the image are determined as their brightness values. Since the bruised areas are darker, the particles with lower brightness values have higher fitness values.

The fitness value of the solution, $fit_m\,(\overrightarrow{x_m})$, is calculated by using the following formula for minimization problems:

$$fit_m\,(\overrightarrow{x_m}) = \begin{cases} \frac{1}{1+f_m(\overrightarrow{x_m})} & f_m\,(\overrightarrow{x_m}) \geq 0 \\ 1 + abs\,(f_m\,(\overrightarrow{x_m})) & f_m\,(\overrightarrow{x_m}) < 0, \end{cases} \tag{3}$$

where $fit_m\,(\overrightarrow{x_m})$ is the objective function value of the solution x_m. This function determines the color values of pixels with particles.

Step 3: An onlooker bee selects a food source based on the probability values calculated using the fitness values provided by employed bees. The probability value p_m, where x_m is selected by an onlooker bee, is calculated using the expression given in (4):

$$p_m = \frac{fit_m(\overrightarrow{x_m})}{\sum_{m=1}^{SN} fit_m(\overrightarrow{x_m})}. \tag{4}$$

After selecting an x_m food source, a new neighboring food source (v_m) is determined by Eq. (2). As in Step 2, a re-selection is made between x_m and v_m.

Step 4: The employed bees that fail to develop a solution in a certain number of trials become scout bees, which are called unemployed bees who randomly choose food sources. The limit here is predetermined by the user. Then these scouts begin to search for new solutions randomly.

Step 5: Memorize the best solution achieved so far.

Step 6: Go to Step 2 unless the number of iterations equals the maximum iteration number.

In this study, the parameters of maximum iteration number, population size, and limit for the ABC-based iterative thresholding approach were selected as 25, 60, and 600 since they reached the highest success in the implemented experiments, respectively.

3.3.2. PSO-based iterative thresholding approach

PSO is a swarm-based algorithm that simulates the movements of birds and fish moving in swarms for finding food in nature as proposed by Kennedy and Eberhart in 1995. PSO is based on sharing information regarding the social behaviors among individuals. Each individual is called a particle, and a collection of particles is called a swarm. Each particle position is adjusted to the best position by taking advantage of previous position experiences. This process is repeated until reaching a termination criterion, such as the maximum iteration number used in this study [27, 28].

The steps of the PSO-based iterative thresholding approach are listed as follows:

Step 1: Generate the initial swarm with starting position and velocity of the particles created at random coordinates within the gray-scale apple image.

Step 2: Calculate fitness values of all particles in the swarm. This value is the color value of the pixel in the image where the particle is located.

Step 3: The personal best ($pbest$) value of each particle (i) is set as the best fitness value of that particle so far.

Step 4: The best $pbest$ value of the current iteration is set as the global best ($gbest$) value.

Step 5: Update the position and velocity of each particle according to Eq. (5) and Eq. (6):

$$v_i^{k+1} = v_i^k + c_1 rand_1 \left(pbest_i - x_i^k\right) + c_2 rand_2 \left(gbest - x_i^k\right), \tag{5}$$

$$x_i^{k+1} = x_i^k + x_i^{k+1}, \tag{6}$$

where x_i^k is the position and v_i^k is the velocity, and c_1 and c_2 are constants expressing acceleration that moves each particle to the pbest and gbest positions. c_1 allows movement of the particle according to its own experiences, and c_2 allows the movement of the particle according to the experiences of other particles in the swarm. $rand_1$ and $rand_2$ are uniformly distributed random numbers in the range of [0,1].

Step 6: Go to Step 2 unless the number of iterations equals the maximum iteration number.

Step 7: If the maximum iteration number is reached, calculate the average of the brightness values at the end positions of the particles and select this value as the iterative threshold value [19].

In this study, the parameters of maximum iteration number used as the termination criterion and population size for the PSO-based iterative thresholding approach were selected as 25 and 60 since they reached the highest success in the implemented experiments, respectively.

In PSO- and ABC-based approaches, the particles were randomly distributed into pixels of the image. The random distribution of particles made initially in the PSO-based approach is shown in Figure 6.

As shown in Figure 6, 60 particles were randomly distributed to an apple image of 600 x 600 pixels. The brightness values (0–255) of pixels with distributed particles are assigned as the fitness values of the particles. The brightness values of particles were compared, and the particles with lower brightness were accepted as having higher fitness values, and the next steps of both algorithms continued. The averages of the best results

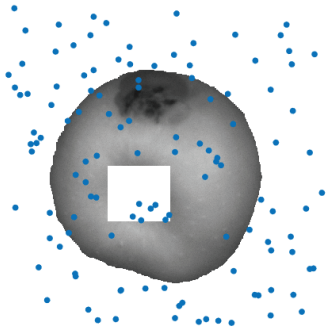

Figure 6. Random distribution of initial particles in PSO-based approach.

of 30 iterations for both approaches were calculated by implementing the algorithms 20 times for each image, and the mean of the average values obtained at the end of 20 repeats was calculated as the threshold value for that image.

4. Results and discussion

When the studies on bruise detection of apples are examined, it is observed that generally hyperspectral or multispectral imaging systems are used in the literature [3, 7, 8]. These systems make it possible to determine the spectral region to facilitate better detection of bruises on apple surfaces. However, these systems are costly and unlikely to be used outside of laboratory environments. Therefore, an image acquisition platform containing an NIR camera was used in the image acquisition stage. The application was run in a MATLAB software environment on a computer with an Intel i7 6700HQ processor and an NVIDIA GeForce GTX 950M graphics card. As a result of the experimental studies, it was determined that the success rate was not very high when the CNN model was used directly for bruise detection. The most important reason for this is the classification of the stem-calyx regions of the apples as bruised. The failure of this situation is shown in Figure 7.

As shown in Figure 7, the major reason for failure to detect the bruised areas of apples is the similarity of the stem-calyx anatomical regions of the apples to the bruised areas. It is seen that especially the calyx region is detected as bruised. For this reason, in our study, first the anatomical regions were detected and discarded from the images, and then the bruised areas were identified by image processing methods. In the CNN model used for detection of the anatomical regions, 80% of the images (960) were used for training, and the remaining 20% (240) were used for testing. The training process lasted about 72 h for 300,000 iterations. Figure 8 shows the images obtained from the application of the CNN model developed for the detection of anatomical regions on the sample apple images.

As shown in Figure 8, an example of raw apple images in the first column was enhanced by using AHE, edge detection, and morphological operations in the 2nd–4th columns. The stem-calyx regions of the image were detected by using the CNN model in the last column. The CNN model developed for the detection of anatomical regions of the sample apple images was successful in distinguishing stem and calyx regions from bruised areas. While selecting sample apple images, all aspects of apples encountered during imaging (bruised/healthy and stem/calyx) were considered. Bruised areas of the images could be more easily segmented by means of the

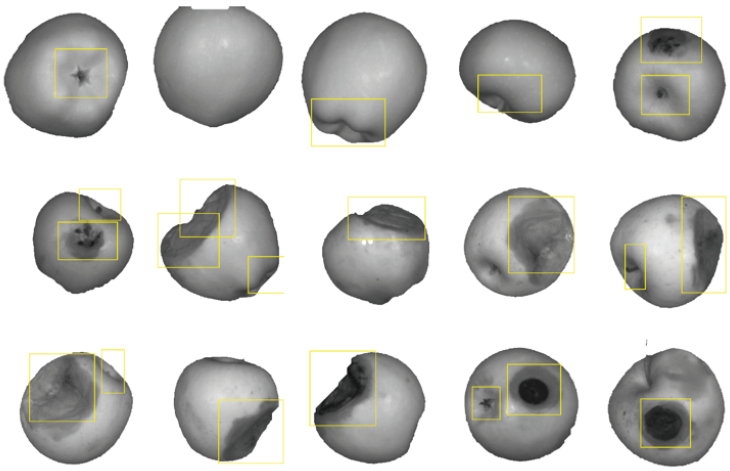

Figure 7. The results obtained by direct application of the CNN model to the apple images.

detection of anatomical regions to be discarded from the image, and so the images with no anatomical regions discarded from the images facilitated the work of the PSO- and ABC-based approaches in the detection of bruised areas. In the PSO-based approach, learning coefficients were taken as 2, and the maximum speed was taken as 30. In the ABC-based approach, the limit parameter was taken as 600 and the acceleration coefficient was taken as 1. The number of iterations in the algorithms was set to 25 and the number of particles was set to 60. These parameters of the algorithms are given in Table 3.

Table 3. ABC and PSO parameters.

Parameters	ABC	PSO
Maximum iteration	25	25
Population size	60	60
Limit	600	-
Acceleration coefficient	1	-
Learning coefficients (c_1, c_2)	-	2
Maximum speed	-	30

In the PSO- and ABC-based approaches, the particles were distributed on random pixels in the image according to the steps of the algorithm. The brightness values of the pixels distributed in the image are determined as the fitness values of the particles. When the particles were compared according to their brightness values, the particles with lower brightness were considered to have higher fitness values. The averages of the results of all iterations were calculated. The presented approaches were repeated 20 times for each image and the mean value of the results was determined as the threshold for that image.

In addition to the ABC and PSO iterative thresholding approaches, Otsu multilevel thresholding was used for the detection of the bruised areas on the images with no stem and calyx regions. Otsu thresholding was implemented at 4 levels, and the threshold values obtained by using Otsu and ABC approaches on the same images are given in Table 4.

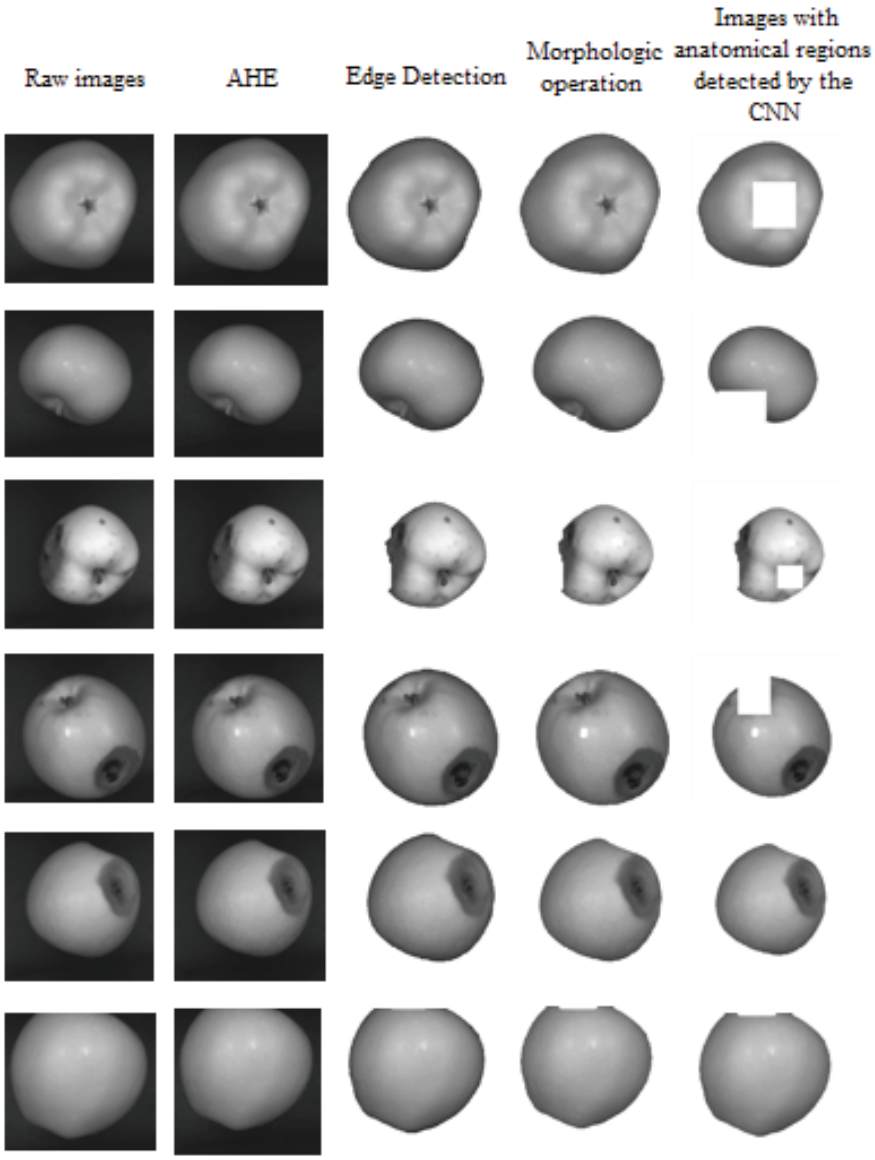

Figure 8. The detection of anatomical areas using the CNN model on the apple images.

In Figure 9, only the smallest of the threshold values determined by using Otsu multilevel thresholding are closer to those determined by using ABC and PSO. The other levels determined by Otsu thresholding do not provide information about the bruised areas. The following figure shows this situation in detail.

As shown in Figure 9, it is evident that the ABC- and PSO-based thresholding is more accurate than the threshold levels determined by using the Otsu approach. Figure 10 shows the images obtained by using the PSO- and ABC-based iterative thresholding approaches on the sample apple images.

As shown in Figure 10, the bruised areas could not be segmented sufficiently well using PSO-based iterative thresholding on apple images. It can be seen that this method usually segmented the healthy areas as bruised. It can be seen that the bruised areas were better detected by using ABC-based iterative thresholding.

Table 4. Results of multilevel thresholding with Otsu.

Image	Otsu	ABC	PSO
1	102, 133, 165, 215	84	86
2	102, 132, 157, 212	86	87
3	104, 152, 191, 232	92	91
4	84, 122, 158, 218	81	95
5	104, 136, 166, 218	81	94
6	103, 133, 165, 218	87	86

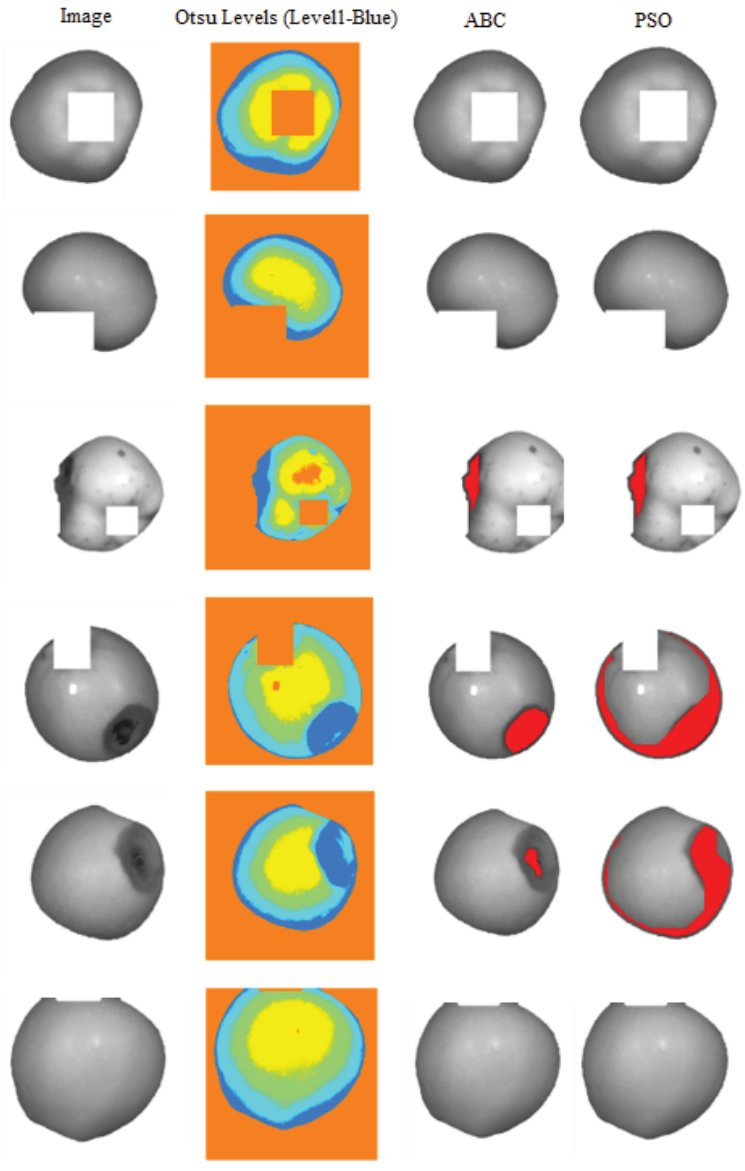

Figure 9. The thresholding results with Otsu, ABC, and PSO on the apple images.

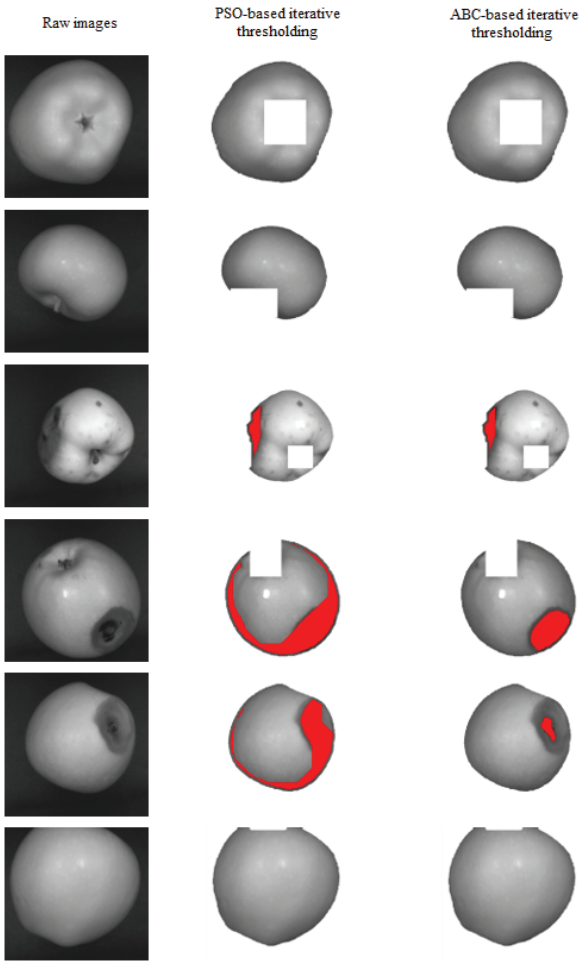

Figure 10. The results obtained by using PSO- and ABC-based iterative thresholding approaches on apple images.

This demonstrates the importance of the values detected in the thresholding that give the best results in all test images. First, the bruised areas of the images were marked by the expert and the bruised area of each image was recorded in pixels. Then, if the ratio of bruised areas of the image to the whole image was more than 15%, the image was labeled as bruised; otherwise, the image was healthy (the expert specified that the ratio between bruised areas and the whole apple image should be 15% so that it could be used directly in fruit juice production). For implementing the classification experiments, according to threshold values determined by using the ABC and PSO approaches, the numbers of pixels of bruised areas were calculated in binary images. According to the calculated values, the ratio of bruised to whole image was calculated, and if this ratio was more than 15%, the image was labeled as bruised; otherwise, the image was labeled as healthy. Then the class labels determined by using PSO/ABC-based iterative thresholding were compared with the class labels recorded by the expert, and then the success ratios of the offered approaches were determined.

In this study, we used the following statistical measures to evaluate the performance of the classification: Specificity: number of true negative decisions (TN)/number of actually negative cases (TN+FP), Sensitivity: number of true positive decisions (TP)/number of actually positive cases (TP+FN), Total correct classification (TCC): number of correct decisions (TN+TP)/number of cases (TN+FN+TP+FP), where sensitivity is the

capacity to find healthy objects among real healthy apples, and it is the ratio of TP decisions to actual positive cases (TP+FN). Specificity is the capacity to find bruised objects among real bruised apples, and it is the ratio of TN decisions to actual negative cases (TN+FP). Total correct classification (TCC) is the ratio of correctly classified decisions (TP+TN) to all cases (TP+FN+TN+FP). Table 5 shows the confusion matrix of the implemented classification with the PSO/ABC-based iterative thresholding approach.

Table 5. The confusion matrix of ABC- and PSO-based iterative thresholding approaches.

	PSO-based iterative thresholding		ABC-based iterative thresholding	
	Healthy	Bruised	Healthy	Bruised
Healthy	722	25	741	11
Bruised	28	425	9	439

As shown in Table 5, when the PSO-based iterative thresholding approach was used, 722 healthy images were classified as healthy objects, 28 healthy images were classified as bruised objects, 25 images with bruised areas were classified as bruised objects, and 425 images with bruised areas with were classified as bruised objects. According to the statistical measures used to evaluate the performance of the classification, sensitivity, specificity, and TCC rates were 93.82%, 96.65%, and 95.58%, respectively. When the ABC-based iterative thresholding approach was used, 741 healthy images were classified as healthy objects, 9 healthy images were classified as bruised objects, 11 images with bruised areas were classified as bruised objects, and 439 images with bruised areas were classified as bruised objects. Accordingly, sensitivity, specificity, and TCC rates were 97.99%, 98.54%, and 98.33%, respectively. The evaluation criteria and the ROC curves of both models are illustrated in Table 6 and Figure 11.

Table 6. Sensitivity, specificity, and TCC rates of ABC- and PSO-based thresholding approaches.

Method	Sensitivity	Specificity	TCC
Thresholding with PSO	93.82	96.65	95.58
Thresholding with ABC	97.99	98.54	98.33

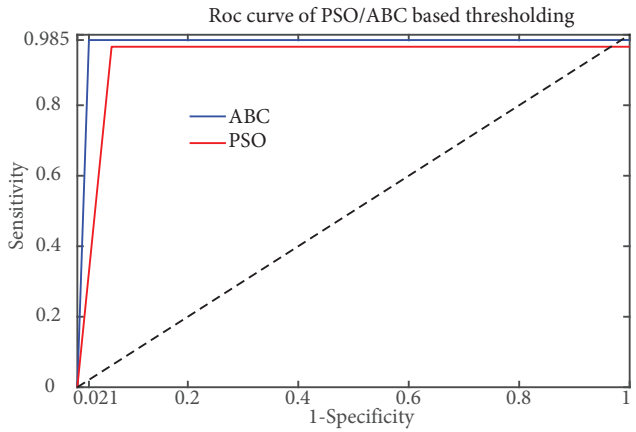

Figure 11. ROC curve of PSO/ABC-based thresholding.

As seen in Figure 11, the ABC-based iterative thresholding approach used was more successful than the other one. In addition, the TP rate in the detection of healthy objects for both methods is actually higher than that of the bruised objects. The specificity of the proposed method was higher than the sensitivity value. The comparison of the success rates of the methods proposed in recent years with respect to bruise detection in apples and the success rates of the proposed methods are given in Table 7.

Table 7. Literature studies on the detection of bruised apples and comparison of the proposed approaches.

Author	Year	Image number	Objective	Method	TCC (%)
Xing and De Baerdemaeker [14]	2005	160	Detection of bruises in apples	Smoothing, thresholding, hyperspectral	86.4
Mohana and Prabhakar [3]	2015	600	Recognition of stem and calyx regions in apples	Multifractal, Fourier, and radon conversions; SVM, ANN, k-NN, LDC, and AdaBoost classifiers	94
Dubey and Jalal [4]	2016	320	Image processing solution for automatic recognition of apple defects	L*a*b* and HSV color spaces, k-means clustering, SVM	93 l
Lu and Lu [5]	2017	120	Detection of bruises in apples	Hyperspectral imaging, opening and filling operations, intermode, Ridler, unimode, and Otsu thresholding	90
Zhang et al. [8]	2017	150	Classification according to the level of bruises in apples	SVM, hyperspectral	92.5
Proposed method-1	2019	1200	Detection of bruises in apples	CNN	74
Proposed method-2	2019	1200	Detection of bruises in apples	CNN+PSO-based iterative thresholding	95.58
Proposed method-3	2019	1200	Detection of bruises in apples	CNN+ABC -based iterative thresholding	98.33

As can be seen in Table 7, when the CNN model (proposed method-1) was used directly for the detection of bruises, the success rate was 74%, not very high. The most important reason for this is that the apple stem-calyx regions were classified as bruised. The classification performances of the ABC- and PSO-based iterative thresholding approaches were compared with those of studies presented in the literature, which used machine learning methods and image processing techniques. The accuracy rates of the methods in our study varied between 95.58% and 98.33%. The success rate of proposed method-3 was 98.33% for apple images whose anatomical regions were discarded by using the CNN model. As a result, the ABC-based iterative thresholding approach produced better results than the PSO-based approach in the detection of bruised areas on apple images.

5. Conclusion

In this paper, we proposed a new model to be used in automatic detection of bruised apples using a hybrid approach, in which the CNN model was used together with an ABC- or PSO-based iterative thresholding approach. Since conventional systems using hyperspectral and multispectral imaging systems that allow the

detection of spectral regions to ensure successful detection of bruised areas in fruit images are both costly and unlikely to be used outside of laboratory environments, we first designed an image acquisition platform with an NIR camera that is both cheap and possible to be used outside of laboratory environments. To be used in the training and testing of our model, 1200 images were taken from 6 different aspects of 200 apples by using this image acquisition platform with NIR camera. These images were enhanced by means of widely used image preprocessing methods. The stem-calyx anatomical regions of the enhanced images were detected by using the CNN model in order to be discarded. A threshold value was determined iteratively by using the ABC/PSO-based iterative threshold approach, the bruised areas of the images were detected, and then the apples were classified according to this determined threshold value. Both ABC- and PSO-based iterative thresholding approaches supported by the CNN model reached satisfactory classification success rates. However, the ABC-based iterative thresholding approach provided a higher classification success rate than the PSO-based iterative thresholding approach in the detection of bruised areas of the apple images. As a result, we believe that the model proposed in this study can be used to automatically separate bruised fruits in the fruit juice industry by means of detecting the bruised areas on them. In future works, it will be possible to develop the bruise segmentation of fruits by increasing the diversity of training data and by using advanced CNN models such as automatic encoders so that real-time bruise detection can be implemented for all fruit types.

Acknowledgment

This work was supported by the Research Fund of Tokat Gaziosmanpaşa University, Project Number: 2016/28.

References

[1] Barrett DM, Somogyi L, Ramaswamy HS. Processing Fruits: Science and Technology. New York, NY, USA: CRC Press, 2004.

[2] Pandey R, Naik S, Marfatia R. Image processing and machine learning for automated fruit grading system: a technical review. International Journal of Computer Applications 2013; 81: 29-39.

[3] Mohana SH, Prabhakar CJ. Stem-calyx recognition of an apple using shape descriptors. Signal and Image Processing International Journal 2015; 5 (6): 17-31.

[4] Dubey SR, Jalal AS. Apple disease classification using color, texture and shape features from images. Signal, Image and Video Processing 2016; 10 (5): 819-826. doi: 10.1007/s11760-015-0821-1

[5] Sa I, Ge Z, Dayoub F, Upcroft B, Perez T et al. Deepfruits: A fruit detection system using deep neural networks. Sensors 2016; 16 (8): 1222. doi: 10.3390/s16081222

[6] Fuentes A, Yoon S, Kim SC, Park DS. A robust deep-learning-based detector for real-time tomato plant diseases and pests recognition. Sensors 2017; 17 (9): 2022. doi: 10.3390/s17092022

[7] Lu Y, Lu R. Histogram-based automatic thresholding for bruise detection of apples by structured-illumination reflectance imaging. Biosystems Engineering 2017; (160): 30-41. doi: 10.1016/j.biosystemseng.2017.05.005

[8] Zhang S, Wu S, Zhang S, Cheng Q, Tan Z. An effective method to inspect and classify the bruising degree of apples based on the optical properties. Postharvest Biology and Technology 2017; 127: 44-52. doi: 10.1016/j.postharvbio.2016.12.008

[9] Zarifneshat S, Rohani A, Ghassemzadeh HR, Sadeghi M, Ahmadi E et al. Predictions of apple bruise volume using artificial neural network. Computers and Electronics in Agriculture 2012; 82: 75-86. doi: 10.1016/j.compag.2011.12.015

[10] Zhihui H, Weiyu Y, Shanxiang L, Jiuchao F. Multi-level threshold image segmentation using artificial bee colony algorithm. Measuring Technology and Mechatronics Automation 2013; 2013: 707-711.

[11] Horng MH. Multilevel thresholding selection based on the artificial bee colony algorithm for image segmentation. Expert Systems with Applications 2011; 38 (11): 13785-13791. doi: 10.1016/j.eswa.2011.04.180

[12] Maitra M, Chatterjee A. A hybrid cooperative–comprehensive learning based PSO algorithm for image segmentation using multilevel thresholding. Expert Systems with Applications 2008; 34 (2): 1341-1350. doi: 10.1016/j.eswa.2007.01.002

[13] Akay B. A study on particle swarm optimization and artificial bee colony algorithms for multilevel thresholding. Applied Soft Computing 2013; 13 (6): 3066-3091. doi: 10.1016/j.asoc.2012.03.072

[14] Xing J, De Baerdmaeker J. Bruise detection on Jonagold apples using hyperspectral imaging. Postharvest Biology and Technology 2005; 37(2): 152-162.

[15] Karaboga D, Akay B. A comparative study of artificial bee colony algorithm. Applied Mathematics and Computation 2009; 214 (1): 108-132. doi: 10.1016/j.amc.2009.03.090

[16] Hao GS, Wang GG, Zhang ZJ, Zou DX. Comparison of PSO and ABC: from a viewpoint of learning. Transactions on Computer Science and Engineering 2017; 2: 108-112. doi: 10.12783/dtcse/aita2017/15999

[17] Le Cun Y, Bottou L, Bengio Y, Haffner P. Gradient based learning applied to document recognition. Proceedings of the IEEE 1998; 86 (11): 2278-2324.

[18] Girshick R. Fast R-CNN. In: Proceedings of the IEEE International Conference on Computer Vision; Santiago, Chile; 2015. pp. 1440-1448.

[19] Adem K. Exudate detection for diabetic retinopathy with circular Hough transformation and convolutional neural networks. Expert Systems with Applications 2018; (114): 289-295. doi: 10.1016/j.eswa.2018.07.053

[20] Lecun Y, Bengio Y, Hinton G. Deep learning. Nature 2015; 521 (7553): 436. doi: 10.1038/nature14539

[21] Karaboga D, Basturk B. A powerful and efficient algorithm for numerical function optimization: artificial bee colony (ABC) algorithm. Journal of Global Optimization 2007; 39 (3): 459-471. doi: 10.1007/s10898-007-9149-x

[22] Otsu N. A threshold selection method from gray-level histograms. IEEE Transactions on Systems, Man and Cybernetics 1979; 9 (1): 62-66.

[23] Onen U, Cakan A, Ilhan I. Performance comparison of optimization algorithms in LQR controller design for a nonlinear system. Turkish Journal of Electrical Engineering and Computer Sciences 2019; 27 (3): 1938-1953. doi: 10.3906/elk-1808-51

[24] Makas H, Yumusak N. Balancing exploration and exploitation by using sequential execution cooperation between artificial bee colony and migrating birds optimization algorithms. Turkish Journal of Electrical Engineering and Computer Sciences 2016; 24 (6): 4935-4956. doi: 10.3906/elk-1404-45

[25] Guvenc U, Isik AH, Yigit T, Akkaya I. Performance analysis of biogeography-based optimization for automatic voltage regulator system. Turkish Journal of Electrical Engineering and Computer Sciences 2016; 24 (3): 1150-1162. doi: 10.3906/elk-1311-111

[26] Karakuzu C. On the performance of newsworthy meta-heuristic algorithms based on point of view fuzzy modelling. Turkish Journal of Electrical Engineering, Computer Sciences 2017; 25 (6): 4706-4721. doi: 10.3906/elk-1705-337

[27] Kennedy J, Eberhart R. Particle swarm optimization (PSO). In: Proceedings of the IEEE International Conference on Neural Networks; Perth, Australia; 1995. pp. 1942-1948.

[28] Adem K, Hekim M, Demir S. Detection of hemorrhage in retinal images using linear classifiers and iterative thresholding approaches based on firefly and particle swarm optimization algorithms. Turkish Journal of Electrical Engineering and Computer Sciences 2019; 27 (1): 499-515. doi: 10.3906/elk-1804-147